SEISMIC BEARING CAPACITY ANALYSIS OF REINFORCED SOILS BY THE METHOD OF STRESS CHARACTERISTICS[*]

A. KESHAVARZ,[**1] M. JAHANANDISH[2] AND A. GHAHRAMANI[2]

[1]School of Engineering, Persian Gulf University, I. R. of Iran
Email: keshavarz@pgu.ac.ir , amin_keshavarz@yahoo.com
[2]Dept. of Civil Engineering, School of Engineering, Shiraz University, I. R. of Iran

Abstract– The ultimate bearing capacity of strip foundations situated on reinforced soils has been analyzed in this paper using the stress characteristics method. A computer code has been written to analyze the slip line net and to calculate the ultimate load distribution beneath the foundation. The ultimate bearing capacity is expressed in terms of bearing capacity factors. Increase in the ultimate bearing capacity due to reinforcement is expressed by introducing another bearing capacity factor, N_t. Earthquake effect has been considered using horizontal and vertical pseudo-static seismic coefficients, K_h and K_v. Design charts have been provided giving the bearing capacity factors for the seismic case. These charts can be used for design purposes for reinforced soils. However, the obtained results should be further compared with future experimental results in order to attain greater confidence in design. Effects of reinforcement and horizontal earthquake coefficient on the failure pattern have also been investigated.

Keywords– Reinforced soil, bearing capacity, strip footing, stress characteristics

1. INTRODUCTION

Strip foundations are used in many structures and calculating the bearing capacity of these foundations is a concern for civil engineers. Reinforcing the soil by adding sheets of geotextiles or geogrids is one idea to increase the bearing capacity of foundations. In seismic areas the bearing capacity problem is more important.

Increasing the bearing capacity of foundations by placing horizontal layers of reinforcement in soil has been demonstrated in several experimental studies (e.g. [1-7]). Huang and Menq [8] used the results of model tests and proposed an equation for the calculation of ultimate bearing capacity of sandy ground reinforced with horizontal stiff reinforcement.

Stress characteristics or slip line method has been used to analyze the behavior of reinforced soils (e.g. [9-13]). In this method the homogenization technique is used and the soil and reinforcement are modeled as a homogeneous-anisotropic material. The advantage of this method is that seismic pseudo-static earthquake coefficients can be applied and the results of the analyzes can be expressed in terms of non-dimensional graphs used in design. Jahanandish and Keshavarz [14] used the method of characteristics to analyze seismic bearing capacity of foundations on reinforced cohesionless soil slopes and provided design charts for practical purposes. Zhao et al. [15, 16] and Zhao [17] used the slip line method for calculating the bearing capacity of reinforced strip foundations. Lesniewska and Porbaha [18] used the method to simulate the behavior of unreinforced and geotextile reinforced retaining walls.

In this paper the method of characteristics has been used to calculate the bearing capacity of foundations situated on reinforced soils in seismic condition. The bearing capacity of foundations on

reinforced soil is expressed as simple bearing capacity factors. Simple design charts have been provided for calculation of the bearing capacity factors under seismic conditions.

2. THEORY

a) The equilibrium-yield equations

Stress characteristics equations for homogeneous perfectly-plastic anisotropic materials have been derived by Booker and Davis [19]. These equations have been derived for the seismic case by Jahanandish and Keshavarz [14] using a different method proposed by Jahanandish [20].

The unknowns of stress tensor in plane strain condition in x-z plane are σ_x, σ_z and τ_{xz} (Fig. 1). If X and Z are body and/or inertial forces in x and z directions, respectively, the equilibrium equations along the characteristics would be:

Along the σ^+ characteristics

$$\frac{dz}{dx} = \tan\left(\psi - m + \mu\right);$$
$$\sin 2(m+\mu)dp + 2Fd\psi = +\cos 2m[(\sin 2\mu dx - \cos 2\mu dz)X \qquad (1)$$
$$+(\cos 2\mu dx + \sin 2\mu dz)Z]$$

and along σ^- characteristics are:

$$\frac{dz}{dx} = \tan\left(\psi - m - \mu\right);$$
$$\sin 2(m-\mu)dp + 2Fd\psi = -\cos 2m[(\sin 2\mu dx + \cos 2\mu dz)X \qquad (2)$$
$$+(\cos 2\mu dx - \sin 2\mu dz)Z]$$

where p is the average stress, $(\sigma_x+\sigma_z)/2$, R is the radius of Mohr circle, and ψ is the angle between x-axis and the direction of major principal stress, σ_1 (Fig. 1) and variables m and μ are defined by:

$$\tan 2m = \frac{1}{2F}\frac{\partial F}{\partial \psi}$$
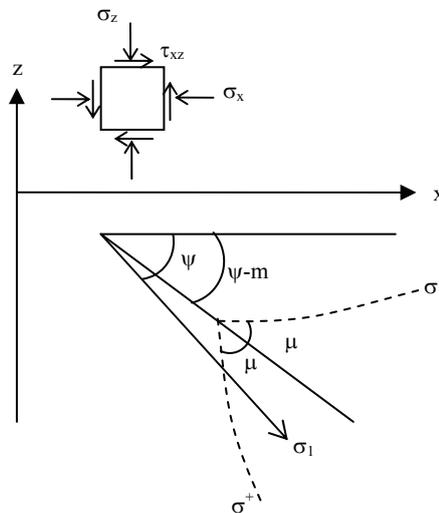$$\cos 2\mu = \cos 2m \frac{\partial F}{\partial p} \qquad (3)$$

Fig. 1. Orientation of σ^+ and σ^- characteristics with respect to x and z axes

The above equations can be obtained from those derived by Booker and Davis [19] if the terms *γcosλ* and -*γsinλ* in their equations are replaced by *X* and *Z*. In these forms of equations, *X* and *Z* are not just the gravity forces, they also include the inertial forces due to earthquake. If the seismic coefficients of earthquake along *x* and *z* are K_h and K_v respectively, then $X = \gamma K_h$ and $Z = \gamma(1 - K_v)$, where *γ* is the unit weight of soil. It should be noted that for the special case of no reinforcement, *m* is zero and *μ* is $45 - \phi/2$, where *φ* is the friction angle of soil. In this case, when earthquake coefficients are zero, these equations reduce to those obtained by Sokolovski [21]. The value of K_v and K_h can be positive or negative and in each case the worst case should be chosen.

Writing Eqs. (1) and (2) in finite difference form, one can compute *x*, *z*, *p* and *ψ* at any point C, when these values are known at points A and B (Fig. 2).
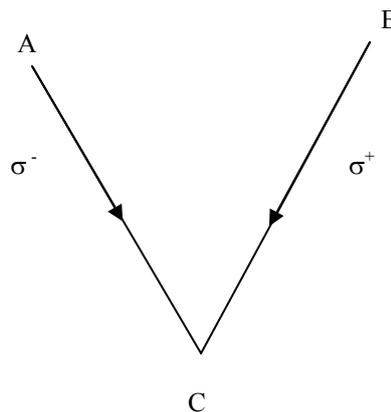

Fig. 2. Information at point C as obtained from A & B along the characteristics

b) Failure criterion

The failure criterion for reinforced cohesive soil has been presented by Michalowski and Zhao [11]. If the layers of reinforcement are placed horizontally and *T* is the resistive force of reinforcement per unit length in *y* direction, assuming *d* to be the vertical distance between the layers, the macroscopic tensile strength of the composite per unit cross section can be expressed by K_t, where:

$$K_t = \frac{T}{d} \tag{4}$$

For reinforcing bars or strips, K_t can be taken as $K_t = T/d_1d_2$ where *T* is the tensile limit force of a single strip or bar and d_1 and d_2 are horizontal and vertical spacings.

The friction angle (*φ*) and cohesion (*c*) of soil are assumed to be constant. The failure criterion would be a function of *ψ* so that:

$$R = p\sin\phi + c\cos\phi \tag{5}$$

when: $\left|2\psi\right| \le \dfrac{\pi}{2} - \phi$;

and,

$$R = \frac{p\sin\phi + c\cos\phi}{\sin(2\psi + \phi)} \tag{6}$$

when: $\dfrac{\pi}{2} - \phi < \left|2\psi\right| \le \dfrac{\pi}{2} - \phi + \tan^{-1}\left(\dfrac{0.5K_t}{p\tan\phi + c}\right)$;

and,

$$\frac{R}{K_t} = -0.5\cos 2\psi + \sqrt{\left(\left(\frac{p}{K_t}+0.5\right)\sin\phi+\frac{c}{K_t}\cos\phi\right)^2 - 0.25\sin^2 2\psi} \tag{7}$$

when: $\dfrac{\pi}{2} - \phi + \tan^{-1}\left(\dfrac{0.5K_t}{p\tan\phi+c}\right) < |2\psi| \le \pi$

c) Boundary conditions along the ground surface

Figure 3 shows a typical stress characteristics field. q is the surcharge and q_f is the ultimate bearing pressure beneath the foundation. At the boundary OD, the values of x and z are known and p and ψ are unknown. No force is mobilized in the reinforcement at this boundary. Therefore the boundary conditions are similar to unreinforced soil. The normal and shear stresses at OD are:
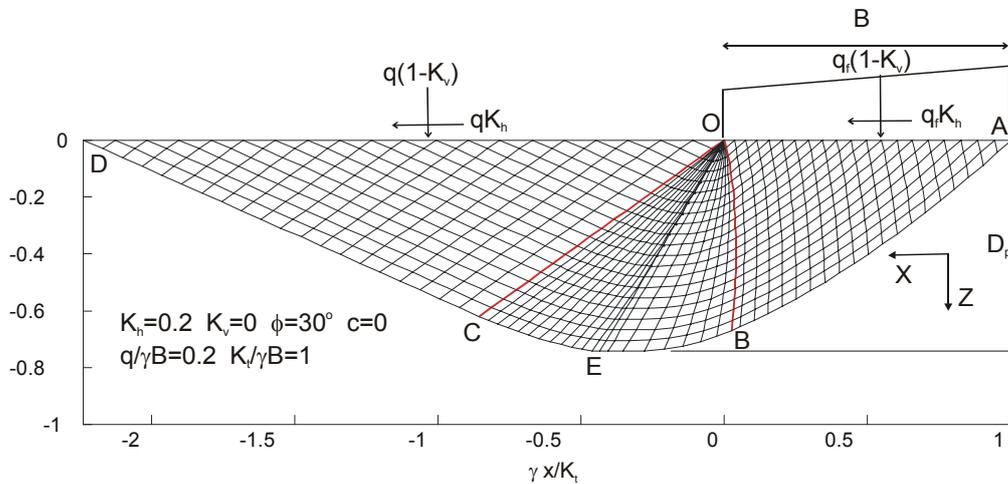
$$\sigma_0 = q(1-K_v), \quad \tau_0 = qK_h \tag{8}$$

Fig. 3. A typical stress characteristics field for reinforced soil

It can be shown that the angle ψ at this boundary is (see Appendix 1):

$$\psi_0 = 0.5\left(\sin^{-1}\left(p_0\sin\delta/R_0\right)-\delta\right) \tag{9}$$

where

$$\delta = \tan^{-1}\left(\frac{K_h}{1-K_v}\right) \tag{10}$$

and p_0 and R_0 are the average stress and radius of Mohr circle at OD, respectively. In the Mohr-circle of stress it can be seen that:

$$R_0{}^2 = \left(p_0-\sigma_0\right)^2 + \tau_0{}^2 \tag{11}$$

Using Eqs. (5), (8) and (11), the value of p_0 can be obtained at this boundary as:

$$p_0 = \frac{\sigma_0 + c\cos\phi\sin\phi + \sqrt{\Delta}}{\cos^2\phi} \tag{12}$$

where

$$\Delta = \left(\sigma_0\sin\phi + c\cos\phi\right)^2 - \tau_0{}^2\cos^2\phi$$

If $K_h = K_v = 0$ (the static case), then $\psi_0 = 0$ and

$$p_0 = \frac{q + c \cos \phi}{1 - \sin \phi} \tag{13}$$

d) Boundary conditions along footing-soil interface

The normal and shear stresses at the boundary OA are:

$$\sigma_f = q_f (1 - K_v), \quad \tau_f = q_f K_h \tag{14}$$

and ψ can be found similar to the boundary OD as (see Appendix 1):

$$\psi_f = 0.5 \left(\pi - \sin^{-1} \left(p_f \sin \delta / R_f \right) - \delta \right) \tag{15}$$

where p_f and R_f are the average stress and radius of Mohr circle for points at OA, respectively. Knowing ψ_f, R_f and p_f, the ultimate pressure q_f, can be found at this boundary as:

$$q_f = \frac{p_f - R_f \cos 2\psi_f}{1 - K_v} \tag{16}$$

e) Analysis procedure

Detailed information about solving the problem can be found in Keshavarz [22]. The procedure is similar to the traditional stress characteristics or slip line method. Knowing p and ψ at the boundary OD, the network of the characteristics in the zone OCD can be obtained using Eqs. (1) and (2) in the finite difference form. Since the angle ψ in the left and right of point O is different, a singularity exists at this point. To solve the net in the zone OCB, the singularity must be solved first.

At the singularity point, $dx = dz = 0$. Therefore, Eq. (2) can be written as:

$$\sin 2 (m - \mu) dp + 2F d\psi = 0 \tag{17}$$

The value of F depends on the values of p and ψ and changes from left to right. Therefore, Eq. (17) should be solved by the numerical procedure, written in the finite difference form.

At the boundary OA, ψ depends on p. Since at point O the failure criterion changes incoming from left to right and ψ_f and p_f are unknown at the right side of O, the equation at the singularity point must be solved by iteration. In solving the equation, first an amount of ψ_f is assumed for the right side of O, and the equation is solved and a new ψ_f is obtained. If the difference between the new and the last one is not small enough, the equation is solved using the new value of ψ_f. This procedure is repeated until the difference between the new and old values of ψ_f is small enough.

Knowing the information at the singularity point O and the line OC, the net in the region OCB can be obtained. Using the information on the line OB, the net of zone OAB can be obtained and the stress field is also determined. At the boundary OA, z is known and p, ψ and x are unknown. Knowing the relationship between p_f and ψ_f at this boundary and the information at the neighbor points on the minus characteristics, the pressure distribution under footing can be obtained. The bearing capacity of soil can then be found by averaging this pressure.

No force is mobilized in the reinforcement in the region ODE. Beyond the characteristic OE, a tensile force is mobilized, but not to the yield value, K_t. A stress discontinuity occurs along OE (see [11] for details). This type of discontinuity was first reported by Rice [23].

3. RESULTS

A computer code has been written for the analysis. Knowing the properties of the soil and reinforcement and the boundary conditions of the problem, the problem can be solved by the code and a plot of the net is obtained. The distribution of the ultimate load under footing is also determined and the average bearing capacity of soil is computed. If $K_t=0$, the program computes the bearing capacity of unreinforced soil.

The distribution of the ultimate load q_f beneath the footing is not always uniform and it depends on the soil and reinforcement parameters. Figure (4) shows a typical distribution of the ultimate bearing pressure for different values of horizontal earthquake coefficient. It can be seen that the values of q_f decrease with increase in K_h. The ultimate bearing capacity, q_u, is obtained by averaging this pressure.
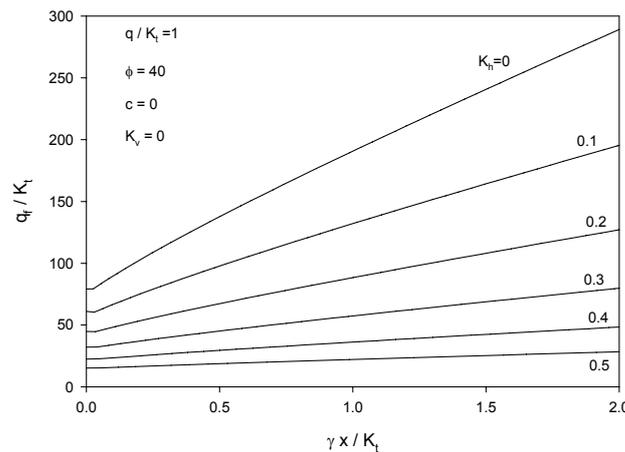

Fig. 4. Typical ultimate load distributions beneath the foundation

a) Bearing capacity of reinforced soil

The ultimate bearing capacity of a reinforced soil can be written as:

$$q_u = cN_c + qN_q + 0.5\gamma BN_\gamma + K_t N_t \tag{18}$$

where the last term accounts for the increase in bearing capacity due to reinforcement. Despite this, it should be mentioned that the effect of reinforcement cannot be found simply by eliminating the other terms in Eq. (18). The failure criterion changes from left to right at the singularity, making derivation of a general explicit expression for N_t difficult. The following expression has been suggested (obtained) by Michalowski [24], Kulczykowski [25] and Sawicki and Lesniewska [13] for the static case when the soil weight is ignored. For other special cases as retaining walls, derivation of a similar formula is also possible.

$$N_t = \left(1 + \sin\phi\right)\exp\left(\left(\frac{\pi}{2} + \phi\right)\tan\phi\right) \tag{19}$$

In the work done here, an indirect procedure has been employed for the determination of N_t. First, a small amount of cohesion or surcharge is assumed and the bearing capacity of unreinforced soil is obtained ($K_t=0$). Second, the bearing capacity of reinforced soil with K_t is determined under the same soil conditions and footing width. The difference is considered as the contribution due to reinforcement, i.e.; the term $K_t N_t$. Analyses for different values of K_t will allow a non-dimensional plot of $K_t N_t / \gamma B$ versus $K_t / \gamma B$ to be constructed. Typical diagrams for $\phi=30°$ and $\phi=40°$ are shown in Figs. (5-6). Lines fitted to the data points indicate a linear relationship between $K_t N_t / \gamma B$ and $K_t / \gamma B$ for each K_h. The slopes of these lines represent the values of N_t as function of ϕ and K_h. Such a result is plotted in Fig. 7. The results

for the static case (K_h=0) have been compared with the suggestion of Michalowski i.e.; Eq. (19) in Fig. 8. The values of N_t obtained in this work are generally higher than those obtained by Eq. (19). Although the difference increases with increase in ϕ, it is below 10% for the practical range of values of the friction angle.
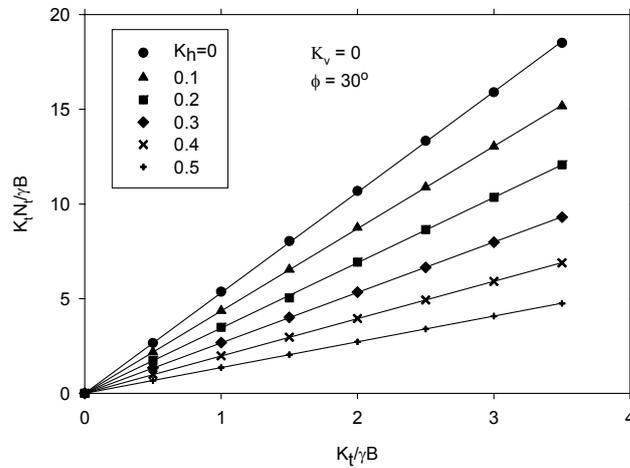

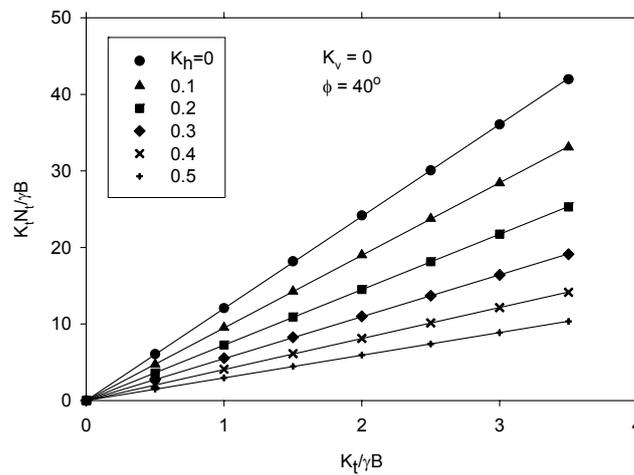Fig. 5. Typical relation between $K_t/\gamma B$ and $K_t N_t/\gamma B$ for different values of K_h (ϕ=30°)

Fig. 6. Typical relation between $K_t/\gamma B$ and $K_t N_t/\gamma B$ for different values of K_h (ϕ=40°)
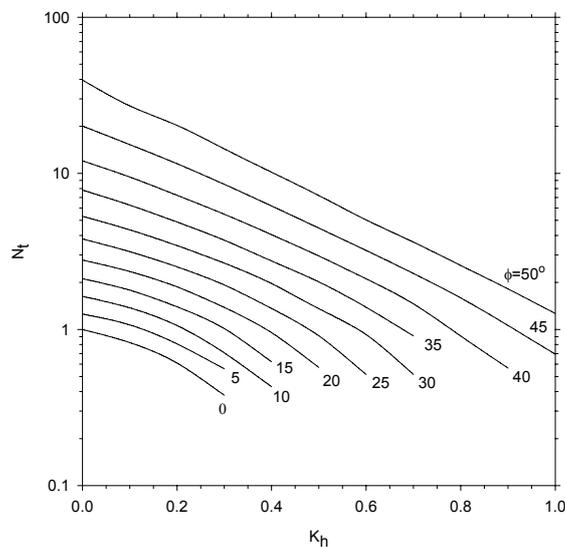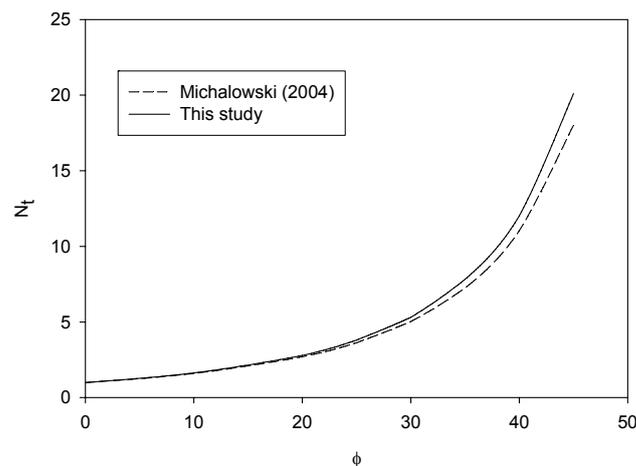

Fig. 7. Bearing capacity factor N_t

Fig. 8. Comparison of N_t between the results of this study and Michalowski [24]

Results of similar analysis for different ϕ and K_h values have been demonstrated in Fig. 7. Using this chart, the value of N_t can be obtained if the friction angle and seismic coefficient are known. As seen, N_t is higher for more frictional soils but generally decreases with an increase in the seismic coefficient.

For simultaneous effect of horizontal and vertical earthquake coefficients, the exact value cannot be obtained from Fig. 7. However, a safe value can be obtained using $K_h/(1-K_v)$ instead of K_h, where K_v is the absolute value. The exact value of bearing capacity in this case can be obtained using the computer code.

Another problem in the design of reinforced foundations is the determination of the depth to which the reinforcement is needed. This requires other considerations like settlement and deformation analysis. But it can be concluded here that the reinforcement must be at least extended to the maximum depth of failure pattern, D_p (Fig. 3). The extent of the plastic zones for $\phi=35^o$, $c=0$, $q/\gamma B=1$ and $K_v=0$ is shown in Fig. 9. As seen, the maximum D_p is obtained when the static case is considered and by increasing K_h, the plastic zone under footing becomes smaller in size. The shrink in the size of the plastic zone with increase in K_h is something that happens in the case of unreinforced soil, as well. In the extreme case when K_h is equal to $\tan\phi$ i.e., the friction coefficient of a frictional soil, the plastic zone shrinks to a line under the base of footing, indicating slippage of footing on soil along the horizontal direction. Due to this fact and because the seismic loading condition is a transient one, we recommend using the higher D_p values obtained from the static case for design. Figure 10 shows the extent of the plastic zone for different values of $K_t/\gamma B$ when $\phi=30^o$ and $K_v=K_h=0$. As shown, the plastic zone enlarges with an increase in K_t. A reinforcement of $K_t/\gamma B=10$ increases D_p by about 16.5% with respect to the unreinforced case. Only 4.5% increase in D_p is obtained if $K_t/\gamma B$ is increased by the same amount, i.e., for $K_t/\gamma B=20$. Therefore, the enlargement of the plastic zone due to reinforcement is not unlimited. For most practical purposes this increase in D_p due to reinforcement is well below 30 to 50%, so that an average factor of 1.4 is enough to be multiplied by the D_p of the unreinforced case of Fig. 11 to cover the required depth of reinforcement for all practical purposes. Figures 11 and 12 show the variation of the maximum depth of failure zone in unreinforced soil for $K_h=0$ and $K_h=0.2$ in non-dimensional form. As shown, D_p increases with the increase in the soil friction angle. The rate of this increase is higher for small values of $\gamma B/(q+c\cot\phi)$. The depth D_p decreases with the increase in K_h (Compare Fig. 11 and Fig. 12). The maximum depth of failure zone shows little increase for reinforced soil. It is obvious that these observations are for the ultimate failure state and a safety factor should be applied for practical purposes.
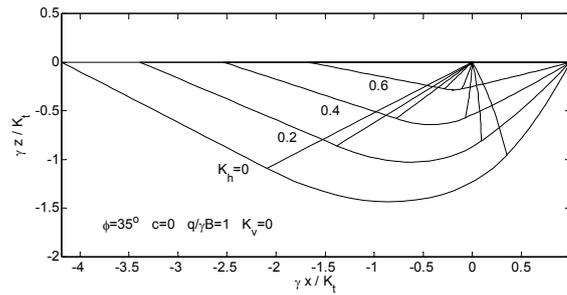
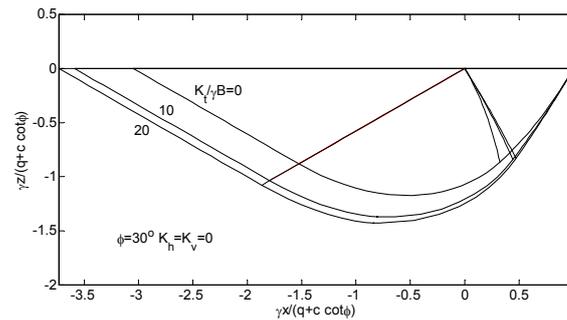Fig. 9. The extent of the plastic zones for different values of K_h

Fig. 10. The extent of the plastic zones for different values of $K_t/\gamma B$
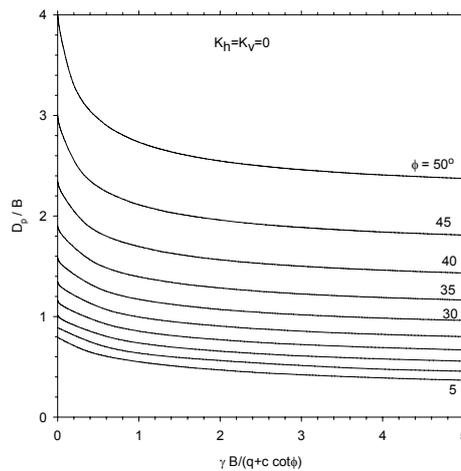

Fig. 11. Variation of maximum depth of failure zones for unreinforced soil in the static case
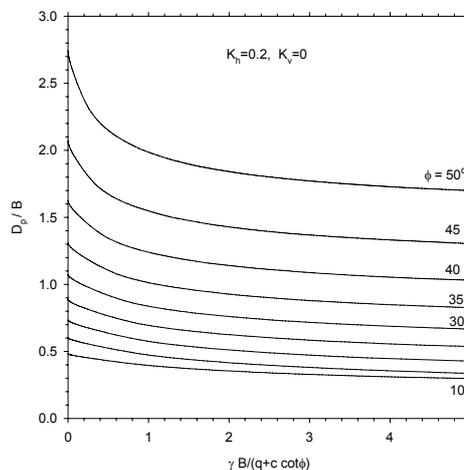

Fig. 12. Variation of maximum depth of failure zones for unreinforced soil (K_h=0.2)

b) Practical applications

   The seismic ultimate bearing capacity of strip foundations on reinforced soil can be calculated using Eq. (18) and Fig. 7. For unreinforced soil, K_t=0. Equations (18) and (4) can be used for the design of reinforcement beneath strip footings (reinforcing materials, spacing …). The soil and reinforcement are assumed homogeneous. Given the width of the footing, soil and reinforcement parameters, the ultimate bearing capacity can be obtained from Eq. (18). If the required ultimate bearing capacity and footing width are known and the necessary reinforcement is to be determined, the value of K_t can be found from Eq. (18). The necessary reinforcement spacing or tensile strength can then be obtained from Eq. (4). However, if the soil and reinforcement parameters are known and footing width is to be determined, an iterative procedure should be employed using Eq. (18). It is necessary to note that in this analysis it is assumed that the reinforcement has enough length so that no slip failure occurs.

   The required least depth for the reinforcement, D_p, is obtained from the geometry of the plastic zones (Fig. 3). This depth can be obtained using Fig. 11 and a proper safety factor. The exact value of ultimate bearing capacity can be calculated using the computer code.

   In the region ODE (Fig. 3) the reinforcement is in compression. No tensile strength of reinforcement is mobilized in this region. The value of the angle between the line OE and vertical axis is about the friction angle of the soil, ϕ [11], and the depth of point E is almost the same as D_p. Therefore, the minimum required length of reinforcement is twice the horizontal distance from point E to A plus the required pullout length as:

$$L_{\min} = 2\left(0.5B + D_p \tan\phi + \frac{T}{2\alpha_b \left(\gamma D_p \left(1-K_v\right)+q\right)\tan\phi} \right) \tag{20}$$

Or

$$\left(L/B\right)_{\min} = 2\left(0.5 + \frac{D_p}{B}\tan\phi + \frac{T}{2B\alpha_b \left(\gamma D_p \left(1-K_v\right)+q\right)\tan\phi} \right) \tag{21}$$

   In the above equations, α_b is a dimensionless reinforcement interaction coefficient value which is less than or equal to 1 [26]. Cohesion between reinforcement and soil is ignored in these equations to give higher length for safety.

   Two examples are provided here to illustrate how the design charts are used:

Example 1. Assume a strip foundation with 1.5m width. The unit weight and friction angle of the cohesionless soil are 18 kN/m^3 and 35°, respectively. The reinforcement used is a strip reinforcement with a tensile limit force of 50 kN/m (for single strip) and vertical distance of 0.5 m. The horizontal distance between the strips is 1 m. The surcharge is 18 kN/m^2. The ultimate bearing capacity for the static case can be calculated as follows:
$K_t = T/\left(d_1 d_2\right) = 50/\left(0.5\times 1\right) = 100\text{kN/m}^2$. For ϕ=35°, N_γ=36.2, N_q=33.3. Here, these bearing capacity factors are obtained by the stress characteristics method. But one can also use the traditional equations to compute these factors. From Fig. 7, N_t=7.8. The ultimate bearing capacity can be calculated using Equation (18) as:

$$q_u = 0+18\times 33.3+0.5\times 18\times 1.5\times 36.2+100\times 7.8 = 1868 \text{ kN/m}^2$$

The exact value of ultimate bearing capacity using the numerical code is 2069 kN/m^2 which is 10% higher than the results of Eq. (18). The value of $\gamma B/\left(q+c\cot\phi\right)$ is 1.5 and, from Fig. 11, D_p/B=1.33.

Therefore, D_p=2 m and 4 layers of reinforcement is required. Using Eq. (20), L_{min}=5.8 m. The exact D_p obtained using the computer code is 2.2 m which is very close to the results of Fig. 11. The ratio of this exact value to that of the unreinforced case obtained from Fig. 11 for this case is 2.2/2.0=1.1, which is well below 1.4, the safety factor recommended to cover most practical purposes.

Example 2. For a strip footing of $B = 2$m on a frictional soil of $\gamma = 19$ kN/m³ and $\phi = 30^o$ when $q = 12$ kPa, the required geogrid of tensile strength $T = 31$ kN/m when $K_h = 0.3$ and $K_v = 0$, can be obtained as the following:

If $\alpha_b = 0.9$ and the required ultimate bearing capacity q_u is 450 kPa. Then N_q=7.5 and N_γ=2.4. Therefore the ultimate bearing capacity of unreinforced soil would be:

$$q_u = cN_c + qN_q + 0.5\gamma BN_\gamma = 0 + 12 \times 7.5 + 0.5 \times 19 \times 2 \times 2.4 = 135.6 \text{ kPa} \prec 450 \text{ kPa}$$

The ultimate bearing capacity of unreinforced soil is smaller than the required one. Therefore, reinforcement is required. From Fig. 7, $N_t = 2.7$. From Eq. (18): $K_t N_t = q_u - (cN_c + qN_q + 0.5\gamma BN_\gamma) = 450 - 135.6 = 314.4 kPa$.

Therefore, K_t=314.4/2.7=116.4 kPa. Now the vertical distance between the reinforcement layers can be calculated using Eq. (4):

$$d = \frac{T}{K_t} = \frac{31}{116.4} = 0.266 \text{ m}$$

From Fig. 11, D_p/B=1, so that D_p=2 m. The required number of reinforcement layers would be 2/0.266=7.5. Taking 8 layers, the new spacing between layers would be 2/8=0.25 m. The minimum length of reinforced layers can also be calculated using Eq. (20) as L_{min}=7.5 m.

For K_t=T/d=31/0.25=124 kPa, the exact ultimate bearing capacity obtained from the computer program is q_u=504.2 kPa, which is greater than the required one (450 kPa). Hence, the results obtained from the design charts are on the safe side. Similarly, the exact value of D_p using the numerical code and is 1.32 m, and is smaller than the result from Fig. 11.

4. CONCLUSION

The method of characteristics has been used to calculate the bearing capacity of strip foundations on reinforced soils. Earthquake effect has been considered as the horizontal and vertical pseudo-static seismic coefficients. A computer program has been written for the analysis. Given the soil and reinforcement parameters and boundary conditions, the program can obtain the net, the failure pattern and the ultimate bearing capacity of the foundation.

Bearing capacity of the reinforced foundations has been expressed in the form of bearing capacity factors. Increase in the ultimate bearing capacity due to reinforcement is expressed by another bearing capacity factor called N_t.

Design charts have been provided for practical applications. Using these charts the ultimate bearing capacity of strip foundations on the reinforced soils can be obtained as well as the required least length and depth of reinforcement. Effects of the reinforcement and horizontal earthquake coefficient on the failure pattern have also been investigated.

REFERENCES

1. Akinmusuru, J. O. & Akinbolade, J. A. (1981). Stability of loaded footings on reinforced soil. *Journal of Geotechnical Engineering Division, ASCE*, Vol. 107, No. 6, pp. 819-827.

2. Binquet, J. & Lee, K. L. (1975). Bearing capacity tests on reinforced earth slabs. *Journal of Geotechnical Engineering Division, ASCE*, Vol. 101, No. 12, pp. 1241-1255.

3. Giudo, V. A., Chang, D. K. & Sweeney, M. A. (1986). Comparison of geogrid and geotextile reinforced earth slabs. *Canadian Geotechnical Journal*, Vol. 23, pp. 435-440.

4. Huang, C. C. & Tatsuoka, F. (1990). Bearing capacity of reinforced horizontal sandy ground. *Geotextiles and Geomembranes*, Vol. 9, pp. 51-82.

5. Patra, C. R., Das, B. M. & Atalar, C. (2005). Bearing capacity of embedded strip foundation on geogrid-reinforced sand. *Geotextiles and Geomembranes*, Vol. 23, pp. 454-462.

6. Esmaili, D. & Hataf, N. (2008). Experimental and numerical investigation of ultimate load capacity of shell foundations on reinforced and unreinforced sand. *Iranian Journal of Science & Technology, Transaction B, Engineering*, Vol. 32, No. B5, pp. 491-500.

7. Mosallanezhad, M., Hataf, N. & Ghahramani, A. (2010). Three dimensional bearing capacity analysis of granular soils, reinforced with innovative grid-anchor system. *Iranian Journal of Science & Technology, Transaction B: Engineering*, Vol. 34, No. B4, pp. 419-431.

8. Huang, C. C. & Menq, F. Y. (1997). Deep-footing and wide-slab effects in reinforced sandy ground. *Journal of Geotechnical and Geoenvironmental Engineering, ASCE*, Vol. 123, No. 1, pp. 30-36.

9. Sawicki, A. (2000). *Mechanics of reinforced soil*. Balkema, Rotterdam/Brookfield.

10. Michalowski, R. L. & Zhao, A. (1995). Continuum versus structural approach to stability of reinforced soil. *Journal of Geotechnical Engineering, ASCE*, Vol. 121, No. 2, pp. 152-162.

11. Michalowski, R. L. & Zhao, A. (1996). Failure of unidirectionally reinforced composites with frictional matrix. *Journal of Engineering Mechanics, ASCE*, Vol. 122, No. 11, pp. 1086-1092.

12. Zhao, A. (1996). Failure loads on geosynthetic reinforced soil structures. *Geotextiles and Geomembranes*, Vol. 14, pp. 289-300.

13. Sawicki, A. & Lesniewska, D. (1988). Limit analysis of reinforced slopes. *Geotextiles and Geomembranes*, Vol. 7, pp. 203-220.

14. Jahanandish, M. & Keshavarz, A. (2005). Seismic bearing capacity of foundations on reinforced soil slopes. *Geotextiles and Geomembranes*, Vol. 23, No. 1, pp. 1-25.

15. Zhao, A., Rimoldi, P. & Montanelli, F. (1996). Design of reinforced foundations by the slip-line method. *Proc. Of Earth Reinforcement*, Japan, Ochiai, Yasufuku and Omine(eds), Balkema, Rotterdam, pp. 709-714.

16. Zhao, A., Riccutti, A. & Gupta, V. (1998). *Design of geosynthetics reinforced foundations by the slip-line method*. In Geohorizon: State of the art in Geosynthetic Technology. Balkema, Rotterdam, pp. 283-293.

17. Zhao, A. (1998). Slip-Line analyses of geosynthetic-reinforced strip footings. Geosynthetics in foundation reinforcement and erosion control systems, Geotechnical special publication no. 76, ASCE, *Proceedings of sessions of Geo-Congress 98*, USA. pp. 49-61.

18. Lesniewska, D. & Porbaha, A. (1998). Numerical simulation of scaled retaining walls by rigid-plastic approach. *Computers and Geotechnics*, Vol. 23, pp. 113-129.

19. Booker, J. R. & Davis, E. H. (1972). A general treatment of plastic anisotropy under condition of plane strain. *J. Mech. Phys. Solids*, Vol. 20, No. 4, pp. 239-250.

20. Jahanandish, M. (2003). Development of zero extension line method for axially symmetric problems in soil mechanics. *Sciencia Iranica*, Vol. 10, No. 2, pp. 203-210.

21. Sokolovski, V. V. (1960). *Statics of soil media*. Butterworth Scientific Publications, London, UK.

22. Keshavarz, A. (2007). Seismic stability analysis of reinforced soil structures by the method of characteristics. PhD Thesis, Shiraz University, Iran. (In Farsi).

23. Rice, J. (1973). Plain strain slip line theory for anisotropic rigid/plastic materials. *J. Mech. Phys. Solids*, Vol. 21, Vol. 1, pp. 63-74.

24. Michalowski, R. L. (2004). Limit loads on reinforced foundation soils. *Journal of Geotechnical and Geoenvironmental Engineering, ASCE*, Vol. 130, No. 4, pp. 381-390.

25. Kulczykowski, M. (1989). Bearing capacity of foundation situated on reinforced earth (in polish). *Archiwum Hydrotechniki*, Vol. 36, No. 1–2, pp. 121–164.

26. Jewell, R. A. (1996). *Soil reinforcement with geotextiles*. CIRIA Special Publication 123, Thomas Telford, UK.

APPENDIX 1. Calculating ψ at the boundaries

It can be seen from Eqs. (8), (14) that

$$\tan \delta = \frac{K_h}{1 - K_v} = \frac{\tau}{\sigma} = \frac{R \sin 2\psi}{p - R \cos 2\psi} \tag{A.1}$$

Simplifying Eq. (A.1)

$$\sin\left(2\psi + \delta\right) = p \sin \delta / R \tag{A.2}$$

Since in the static case (δ=0), ψ_f=π/2 and ψ_0=0, Eqs. (9) and (15) are obtained from Eq. (23) for the boundaries.